

Investigation of the Nonlinear Interaction between a Fast Ion Beam and Plasma Electrons

M. D. Gabovich, I. A. Soloshenko, and L. S. Simonenko

Institute of Physics, Ukrainian Academy of Sciences

Submitted July 21, 1971

Zh. Eksp. Teor. Fiz. 62, 1369-1375 (April, 1972)

An experimental study has been carried out of the nonlinear interaction between an ion beam and plasma for beam velocities in excess of the thermal velocity of the plasma electrons. As in the case of an electron beam, the restriction on the current oscillation amplitude is connected with the wave inversion in the region of the phase focus. The restriction on the potential oscillation amplitude is connected with another nonlinear mechanism, namely, the capture of the plasma electrons by the wave field. This effect has been detected as a result of a particular feature of the nonlinear interaction between the ion beam and the plasma which ensures the capture of the plasma particles by the wave field before the phase focus in some cases. It is also shown that the nonlinear interaction leads to the heating of the plasma electrons and to beam energy losses.

1. When a monoenergetic charged-particle beam interacts with plasma the main nonlinear effects leading to the restriction in the growth of the wave are wave inversion and wave capture by the potential wells of the beam and plasma particle waves. An analytical study of the nonlinear interaction between an electron beam and plasma was carried out in^[1,2] on the assumption that the beam density was much less than the plasma density, i.e., $(n_1/n_0)^{1/3} \ll 1$. This ensured that effects connected with the capture of plasma electrons by the wave field could be neglected because the depth of the potential well of the wave was much less than the beam energy, i.e., $2e\varphi \ll mv_0^2/2$. The nonlinear interaction has also been investigated both numerically^[3-5] and experimentally.^[6,7] The effects associated with wave inversion and the formation of a multiveLOCITY beam in the region of the phase focus of the beam were established. For high values of n_1/n_0 the computer experiments showed the presence of the capture of plasma electrons by the wave field^[3], which occurred in the region of wave inversion, but in laboratory experiments with electron beams this effect was not detected. In the present paper we report the first experimental study of the nonlinear effects during the excitation of Langmuir electron oscillations in plasma by an ion beam in the case where the beam and plasma densities are comparable. In some cases, this system will exhibit the capture of plasma electrons by the wave field well before the appearance of nonlinear effects in the dynamics of the beam ions, i.e., the condition $2e\varphi \sim mv_0^2/2$, where v_0 is the ion beam velocity, may be satisfied before the phase focus. This fact has enabled us in the present experiments to detect both phase focusing of the ion beam and, for the first time, the capture of plasma electrons by the wave field.

2. The experiments were performed using the apparatus illustrated schematically in Fig. 1. The H_2^+ ions were extracted from the duoplasmatron 1, they were accelerated by the field of the electrode 2, and were then shaped into the parallel beam 4 by the magnetic lens 3. The beam current was usually about 20 mA, the energy was 30 keV, and the particle density 10^7 cm^{-3} . The plasma was produced by the beam as a result of the ionization of the neutral gas. When the pressure was varied from 1×10^{-5} to 5×10^{-4} torr the plasma-electron density was found to vary from 10^7 to 10^8 cm^{-3} .

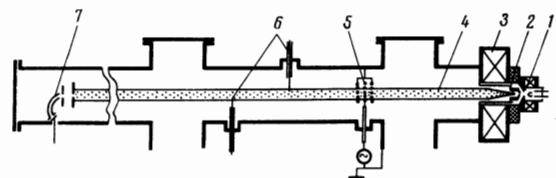


FIG. 1. Schematic of the apparatus. 1—Duoplasmatron ion source, 2—extracting electrode, 3—magnetic lens, 4—ion beam, 5—modulator, 6—probes, 7—ion energy analyzer.

The beam was energy-modulated by means of the three-grid modulator 5 (outer grids grounded, middle grid connected to a high-frequency generator) and then entered the interaction region whose length was $L \sim 500 \text{ cm}$. The analyzer 7, which was located at the end of the chamber, was of the Hughes-Rojansky type and was used for the energy analysis of the ions. The calculated resolving power of the analyzer was $\sim 1\%$. The beam-current oscillations were investigated by using collectors which were screened from the plasma by grounded grids, whereas the potential oscillations were investigated with the insulated probes 6. The electron distribution function was measured with a two-grid analyzing probe which was mounted parallel to the beam.

3. In the absence of external beam modulation the system was found to support Langmuir electron oscillations whose amplitude increased exponentially along the entire chamber.^[8] When the beam was modulated externally the dependence of the oscillation amplitude on the generator frequency was precisely the same as the envelope of the spectrum of the oscillations excited by the unmodulated beam. The oscillation amplitude was a maximum at a frequency roughly equal to the Langmuir frequency of the plasma because the spatial growth rate was then a maximum. Figure 2 shows the experimental dependence of the spatial growth rate γ of the oscillations as a function of the modulation frequency for two values of the neutral gas pressure, i.e., two values of the plasma-electron density.

We note that the external modulation of the ion beam led to the removal of instability at frequencies different from the modulation frequency (as in the case of the electron beam^[9]), and the amplitude of the modulating voltage at which the instability suppression occurred

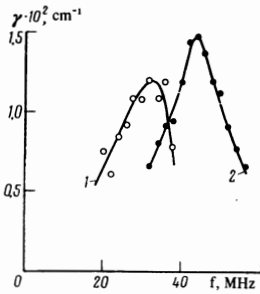


FIG. 2

FIG. 2. Spatial growth rate of the oscillations as a function of modulation frequency. 1— $P = 8 \times 10^{-5}$ torr, 2— $P = 1.2 \times 10^{-4}$ torr.

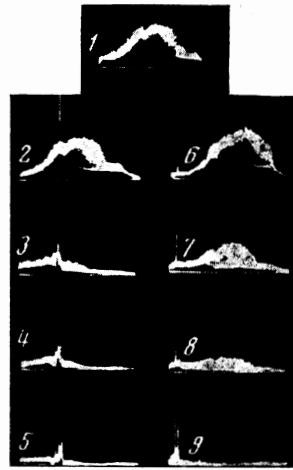


FIG. 3

FIG. 3. Effect of beam modulation on the spectrum of excited oscillations, $P = 8 \times 10^{-5}$ torr. 1—Modulation amplitude $U_1 = 0$, 2— $U_1 = 14$ V, modulation frequency $f = 27$ MHz, 3— $U_1 = 34$ V, $f = 27$ MHz, 4— $U_1 = 50$ V, $f = 27$ MHz, 5— $U_1 = 70$ V, $f = 27$ MHz, 6— $U_1 = 20$ V, $f = 20$ MHz, 7— $U_1 = 50$ V, $f = 20$ MHz, 8— $U_1 = 100$ V, $f = 20$ MHz, 9— $U_1 = 150$ V, $f = 20$ MHz.

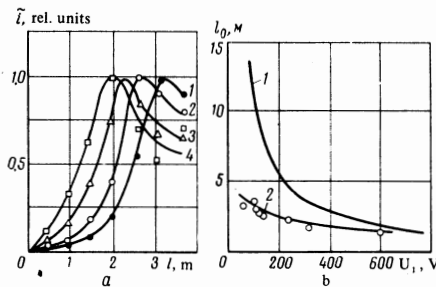


FIG. 4. a—Distribution of the amplitude of the fundamental harmonic of the current along the beam axis, $P = 8 \times 10^{-5}$ torr, $f = 27$ MHz. Curve 1— $U_1 = 60$ V, 2— $U_1 = 120$ V, 3— $U_1 = 240$ V, 4— $U_1 = 360$ V. b—Position of the maximum of the fundamental harmonic of the current as a function of the initial modulation amplitude. Solid curves 1 and 2—calculated, points—experimental.

decreased as the modulation frequency approached the Langmuir frequency.

4. When a sufficiently high alternating voltage from the generator was applied to the modulator we observed nonlinear effects associated with the restricted amplitude of the oscillations. Figure 4a shows the amplitude distribution for the fundamental harmonic of the beam current along the axis of the system for different outputs of the high-frequency generator. It is clear that the oscillation amplitude at first increased and, having reached a maximum, decreased again to some extent. The maximum amplitude of the fundamental harmonic does not depend on the initial modulation level and is roughly equal to the constant component of the current. An increase in the amplitude of the modulating voltage leads only to a reduction in the distance up to the maximum. Analysis of these curves shows that we are observing here phase bunching of the beam ions. Figure 4b shows the calculated positions of the amplitude maxi-

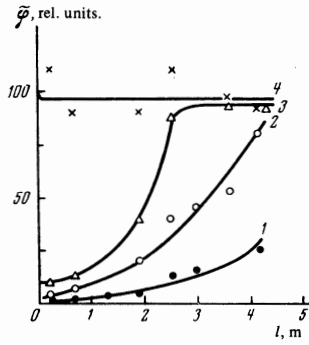


FIG. 5

FIG. 5. Distribution of the fundamental harmonic of the potential along the beam, $P = 8 \times 10^{-5}$ torr, $f = 27$ MHz. Curves 1— $U_1 = 18$ V, 2— $U_1 = 40$ V, 3— $U_1 = 120$ V, 4— $U_1 = 360$ V.

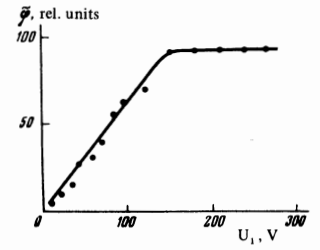


FIG. 6

FIG. 6. Amplitude of the fundamental harmonic of the potential as a function of the modulation amplitude, $P = 8 \times 10^{-5}$ torr, $f = 27$ MHz, $L = 2$ m.

um of the fundamental harmonic of the current as a function of the amplitude of the modulating signal. Curve 1 was calculated from the theory of the kinematic klystron, and curve 2 takes into account the increase in the alternating component of the beam—particle velocity due to the two-stream instability during the interaction with the plasma,^[4] in accordance with the formula

$$(e^{v_0} - e^{-v_0}) / 2\gamma = 3.68v_0U_0 / \omega U_1,$$

where v_0 is the initial velocity of the beam particles, eU_0 is the beam-particle energy, U_1 is the amplitude of the modulating signal, ω is the modulating frequency, and γ is the spatial growth rate of the oscillations. We used in the calculations the experimentally determined value $\gamma \approx 0.01 \text{ cm}^{-1}$. The experimental positions of the maximum of the fundamental harmonic of the current are shown by points in Fig. 4b and are in good agreement with calculations. We note that for large modulation amplitudes, when the distance to the phase focus calculated from the theory of the kinematic klystron is less than the growth length $S_k = 2v_0U_0 / \omega U_1 < 1/\gamma$, the increase in the velocity oscillations due to the interaction with the plasma is not detected and the distance to the maximum is close to the value calculated from the kinematic theory of the klystron. For small modulation amplitudes, when $S_k > 1/\gamma$, the beam-plasma interaction becomes important and the distance to the maximum is much less than the value predicted by the kinematic theory.

5. To investigate the capture of the plasma electrons by the wave field, we measured the amplitude of the oscillations in the potential in the system. Figure 5 shows the amplitude distribution for the fundamental harmonic of the potential along the beam for different output voltages of the high-frequency generator. For small modulation amplitudes the oscillations increase exponentially along the length of the chamber (curves 1 and 2). For high values of U_1 the curves reach saturation at some point along the axis (curve 3), and above a certain value of the modulation voltage a wave growing in space is not observed (curve 4). The nonlinear saturation effects can also be seen in Fig. 6, which shows the amplitude of the fundamental harmonic of the potential as a function

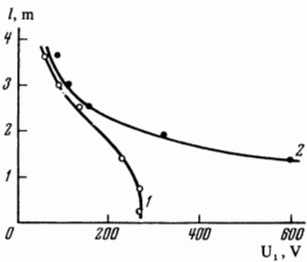


FIG. 7

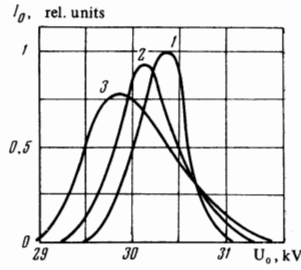


FIG. 8

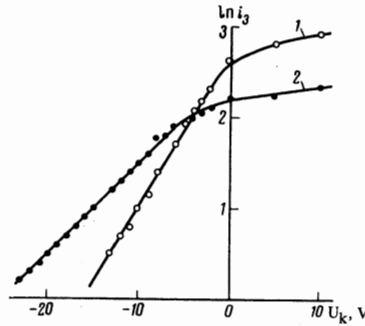


FIG. 9

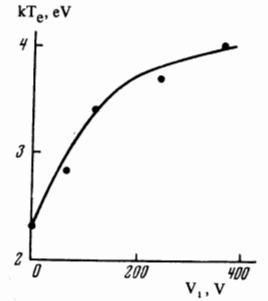


FIG. 10

FIG. 7. Distances at which the fundamental harmonic of the potential (curve 1) and the fundamental harmonic of the current (curve 2) reach their maxima as functions of the modulation amplitude; $P = 8 \times 10^{-5}$ torr, $f = 27$ MHz.

FIG. 8. Ion-energy distribution in the beam. Curve 1— $P = 1 \times 10^{-5}$ torr, unmodulated beam; 2— $P = 8 \times 10^{-5}$ torr, unmodulated beam; 3— $P = 8 \times 10^{-5}$ torr, modulated beam; $U_1 = 150$ V, $f = 27$ MHz.

FIG. 9. Electron temperature as a function of the modulation voltage, $P = 8 \times 10^{-5}$ torr. Curve 1—unmodulated beam; 2—modulated beam; $U_1 = 300$ V, $f = 27$ MHz.

FIG. 10. Electron temperature as a function of the modulation voltage; $P = 8 \times 10^{-5}$ torr, $f = 27$ MHz.

of the modulation amplitude measured at a distance of 2 m from the modulator. The saturation potential is the same at all points along the beam axis.

Figure 7 shows the distance at which the fundamental harmonic of the plasma potential oscillations saturates as a function of the amplitude of the modulating signal (Fig. 1). For comparison, we also show the analogous dependence for the maximum of the beam current (Fig. 2). It is clear that for small modulation amplitudes ($S_k > 1/\gamma$) curves 1 and 2 are practically identical, i.e. the saturation of the fundamental harmonic of the oscillations occurs near the phase focus of the ion beam. For large modulation amplitudes ($S_k < 1/\gamma$) the saturation of the amplitude of the fundamental harmonic of the potential occurs much earlier than the phase focusing of the ion beam. This difference is due to the fact that the restriction on the amplitude of the potential oscillations is, in this case, connected not with the phase focusing of the beam ions but with the capture of plasma electrons by the wave field. To confirm this, let us estimate the amplitude of the fundamental harmonic of the potential in the region of the phase focus, assuming that the modulation amplitudes are small and the wave grows in space exponentially up to the focus, i.e. $\varphi_{ph} = \varphi_1 e^{\gamma l_0}$. In the linear theory, the relation between φ_1 and the amplitude U_1 of the modulating signal is given by $\varphi_1 = \gamma U_1 v_0 / 2\omega$. The position of the phase focus is given by^[5]

$$e^{\gamma l_0} = 4\gamma v_0 U_0 / U_1 \omega.$$

Therefore, $\varphi_{ph} = 2(\gamma v_0 / \omega)^2 U_0$. Under the conditions of our experiment this quantity was $\varphi_{ph} \approx 6$ V. The capture of plasma particles by the wave requires that $\varphi > mv_0^2 / 4e \approx 4$ V. Hence, it is clear that the capture of plasma electrons should, in fact, occur in this case near the phase focus. For large modulation amplitudes, when the potential in the wave is equal to the saturation potential almost immediately after the modulator, the capture of electrons occurs near the modulator and, therefore, the system does not exhibit the exponential growth of the potential oscillations. As already noted, ion bunching then occurs in practically the same way as in the kinematic klystron.

6. We have also measured the time-averaged beam-

ion velocity distributions and plasma-electron velocity distributions. Figure 8 illustrates the effect of oscillations on the ion energy distribution. Curve 1 was obtained at a pressure $P = 10^{-5}$ torr when the growth rate was low, and curve 2 corresponds to $P = 8 \times 10^{-5}$ torr when γ appreciably increases and is roughly 0.01 cm^{-1} . Curve 3 was taken at $P = 8 \times 10^{-5}$ torr but in the presence of the external beam modulation. It is clear that the excitation of the oscillations produces a broadening of the energy distribution function and leads to a loss of energy.

External modulation produces an appreciable reduction in the distribution function only in the case when the modulation frequency is close to the electron Langmuir frequency. The broadening of the distribution function with increasing amplitude of the modulating signal occurs only until the distance to the phase focus remains greater than the length of the apparatus, and further increase in the modulation amplitude has little effect on the width of the distribution function. It is only at very high generator outputs, when the system does not support a growing wave, that the width of the distribution function becomes equal to twice the modulation amplitude. This enables us to conclude that the observed distribution function is the result of an averaging of the beam energy oscillations, just as in the case of the electron beam.^[7] In fact, the observed width of the averaged distribution function is close to twice the amplitude of the beam-energy oscillations in the region of the phase focus calculated on the assumption that the wave grows exponentially up to the phase focus: $2eU = eU_1 e^{\gamma l_0} = 4\gamma v_0 e U_0 / \omega \approx 1200$ eV. The formation of the phase focus (Fig. 5) and the behavior of the average distribution function in themselves support the hypothesis that, as in the case of the electron beam, there is wave inversion and the formation of a multivelocity current in the region of the phase focus.

As expected, the nonlinear interaction between the ion beam and the plasma results in the heating of the electrons. As an illustration, Figure 9 shows on a semi-logarithmic scale the current-voltage characteristics of the analyzing probe for a nonmodulated (curve 1) and a modulated (curve 2) beam. Figure 10 shows the electron temperature determined from the slope of the

straight lines as a function of the amplitude of the modulating signal. It is clear that an appreciable temperature increase is observed when the modulation amplitude is varied from 0 to 200 V. An increase in the generator output has practically no effect on the electron temperature as soon as the amplitude of the potential oscillations has reached saturation along the length of the chamber.

The increase in temperature gives rise to a greater escape of electrons from the beam. If the initial electron density is close to the beam density this leads to a deterioration in the neutralization of the beam space charge, i.e., to an increase in the radial static potential drop and a certain angular divergence. This is in agreement with the results reported in^[10].

7. We have thus shown that: 1) the restriction on the amplitude of the beam current oscillations is connected with phase focusing of the ions; 2) the restriction on the amplitude of the potential oscillations is connected with the plasma-electron capture by the wave field, and 3) the excitation of the oscillations leads to the heating of plasma electrons and to beam energy losses.

¹B. B. Kadomtsev and O. P. Pogutse, On the Theory of the Beam-plasma Interaction, Preprint ic/70/45, Trieste, 1970.

²V. D. Shapiro and V. I. Shevchenko, Zh. Eksp. Teor. Fiz. **60**, 1023 (1971) [Sov. Phys.-JETP **33**, 555 (1971)].

³J. A. Davis and A. Bers, Proc. Symposium on Turbulence of Fluids and Plasmas, Brooklyn, 1968, p. 87.

⁴J. M. Davson, C. G. Hsi, and R. Shanny, Plasma Physics and Controlled Nuclear Fusion Research, Vol. 1, Vienna, 1969, p. 735.

⁵I. M. Gel'fand, I. M. Zueva, V. S. Imshennik, O. V. Loputsievskii, V. S. Ryaben'kii, and L. G. Khazin, Zh. Vychisl. Mat. Mat. Fiz. **7**, 322 (1967).

⁶M. D. Gabovich and V. P. Kovalenko, Zh. Eksp. Teor. Fiz. **57**, 716 (1969) [Sov. Phys.-JETP **30**, 392 (1970)].

⁷M. D. Gabovich and V. P. Kovalenko, Ukr. Fiz. Zh. **15**, 1893 (1970).

⁸M. D. Gabovich and I. A. Soloshenko, Zh. Tekh. Fiz. **41**, 1627 (1971) [Sov. Phys.-Tech. Phys. **16**, 1281 (1972)].

⁹A. K. Berezin, Ya. B. Fainberg, and I. A. Bez'yazychnyi, Zh. Eksp. Teor. Fiz. Pis'ma Red. **7**, 156 (1968) [JETP Lett. **7**, 119 (1968)].

¹⁰M. D. Gabovich, I. A. Soloshenko, and A. A. Ovcharenko, Ukr. Fiz. Zh. **16**, 812 (1971).